The Binding Site of a Specific Aminoglycoside Binding RNA Molecule†

Junhyeong Cho, Keita Hamasaki, and Robert R. Rando*

Department of Biological Chemistry and Molecular Pharmacology, Harvard Medical School, 250 Longwood Avenue, Boston, Massachusetts 02115

Received November 10, 1997; Revised Manuscript Received February 6, 1998

ABSTRACT: A small (40 nucleotides) stem-loop derivative (J6f1) of a specific aminoglycoside-binding RNA aptamer, containing a 3 nt and a 1 nt bulge, has previously been shown to stoichiometrically bind tobramycin with a dissociation constant of approximately 5 nM [Hamasaki, K., Killian, J., Cho, J. and Rando, R. R. (1997) *Biochemistry 36*, 1367−1371]. This construct can strongly discriminate among similar aminoglycosides with respect to binding. A combination of chemical interference studies, chemical modification studies, and mutational studies are performed to define the aminoglycoside binding site of J6f1. Recognition of the aminoglycoside by J6f1 involves contacts with nucleotide bases, rather than with the phosphate backbone. The binding site 1 comprised of part of the stem-loop region. The two bulges are also essential for high affinity and stoichiometric binding of tobramycin. These bulges are probably important for prying open the double helical region, thereby allowing the aminoglycoside access to the nucleotide bases.

Aminoglycosides are important antibiotics used in the treatment of Gram negative infections (*1*). These agents appear to function by binding to the decoding region of prokaryotic 16S rRNA, causing mis-reading of the messenger RNA (*2*, *3*). The binding of aminoglycosides to RNA is, however, not confined to binding to the decoding region. Many naturally occurring RNA species, including group I introns (*4*), a hammerhead ribozyme (*5*), and the RRE transcriptional activator region from HIV (*6*), also bind aminoglycosides. In fact, it is a straightforward matter to carry out in vitro selections against aminoglycosides to generate a variety of RNA aptamers able to bind these antibiotics (*7*−*9*). The various RNA molecules uncovered which bind aminoglycosides show little apparent sequence homology, suggesting that there are many structural solutions available for aminoglycoside binding. However, most of the aminoglycoside-binding RNA molecules described so far appear to bind aminoglycosides in the micromolar range. This level of binding affinity can be very easily obtained. For example, the in vitro selection of RNA aptamers (starting with approximately 10^{14} sequences) against the aminoglycoside tobramycin led to 10^7 sequences which could bind tobramycin with affinities in the low micromolar range (*7*). Of course, no consensus sequences were observed in these weak binders. To obtain strong binders, the weak binding pool was reselected under more stringent conditions, producing high-affinity aptamers with consensus sequences (*7*). One of these aptamers, termed J6 (Scheme 1), bound tobramycin stoichiometrically with a measured dissociation constant (K_D) of 0.77 nM (*7*). The construct was quite specific for tobramycin as well and discriminated among similar aminoglycosides by factors of 10^3−10^4 (*7*).

Scheme 1: Structure of Tobramycin, CRT, and the Minimized 40-Nucleotide RNA Sequence (J6f1)

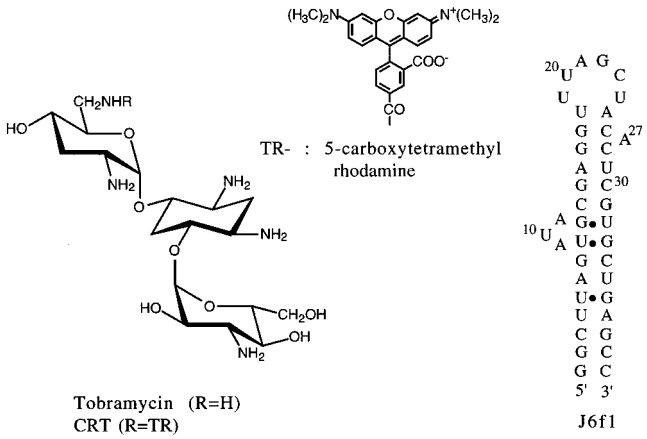

RNA aptamers of the J6 type are exceedingly interesting for possible structural study because of the high affinity and high specificity that they show as aminoglycoside binders. As stated above, micromolar binding affinities for aminoglycosides are relatively commonplace, and it may be difficult to discern discrete modes of RNA-aminoglycoside recognition which might serve as starting points for the design of specific antagonists of particular RNA targets. We have been interested in dissecting the salient aminoglycoside binding core from the 109-mer J6 for further analysis of the binding region. Previously, we had been able to demonstrate that the small construct, J6f1 (Scheme 1) specifically and stoichiometrically binds tobramycin (*10*). Deletion studies demonstrated that the 3 and 1 nt[1] bulges are essential for high-affinity tobramycin binding, as is the integrity of the loop portion of the molecule (*10*). In this article, the structure

† These studies were partially funded by U.S. Public Health Service National Institutes of Health Grants EY-03624 and EY-04096. K.H. was funded by a research fellowship from the Japan Society for the Promotion of Science.

* To whom correspondence should be addressed.

S0006-2960(97)02757-8 CCC: $15.00
Published on Web 03/18/1998

of J6f1 is further probed by chemical and mutational methods to reveal the precise nature of the aminoglycoside binding site.

MATERIAL AND METHODS

Materials. Tobramycin was purchased from Fluka. Diethyl pyrocarbonate (DEPC), hydrazine, and ethyl nitrosourea (ENU) were purchased from Sigma. Cerium(III) nitrate hexahydrate and aniline were purchased from Aldrich. 5-Carboxytetramethylrhodamine labeled tobramycin (CRT) was prepared as previously reported (*11*). Oligonucleotides were obtained from Oligo's, Etc., Inc. PCR reactions were carried out using the Gene Amp PCR kit with AmpliTaq DNA polymerase from Perkin-Elmer. RNA transcripts were generated using the RiboMAX large-scale RNA production kit with T7 RNA polymerase from Promega. *N*-hydroxysuccinimide-derivatized Affi-Gel 10 was from Bio-Rad and Sephadex G-50 was from Pharmacia.

RNA Synthesis and Purification. J6f1 RNA and mutant RNAs were transcribed in vitro by T7 RNA polymerase using synthetic oligonucleotide templates (*12*). All RNA contained GG at the 5′-end to increase the efficiency of transcription. To label RNA at the 5′-end, dephosphorylated RNA was incubated with [γ-^{32}P]ATP and polynucleotide kinase. RNA was purified on 18% polyacrylamide gels and eluted from the gels with 0.3 M NaOAc and 1 mM EDTA (pH = 4.5) and finally precipitated with ethanol. Purified RNA was resuspended in sterile deionized water. The RNA was renatured by incubating in binding buffer (140 mM NaCl, 5 mM KCl, 1 mM $CaCl_2$, 1 mM $MgCl_2$, and HEPES, pH = 7.4) for 1 min at 80 °C followed by slow cooling to 25 °C.

Chemical Modification Interference Assays. 5′-^{32}P-labeled J6f1 RNA (2×10^6 cpm) was mixed with 10 μg of carrier tRNA and modified at less than one site per molecule with diethyl pyrophosphate (DEPC) or hydrazine under denaturing condition as described (*13*). The modified RNA was precipitated with ethanol and renatured in buffer containing 140 mM NaCl, 5 mM KCl, 1 mM $CaCl_2$, 1 mM $MgCl_2$, and 20 mM HEPES (pH = 7.4) by heating to 80 °C for 1 min followed by slow cooling to 25 °C. The RNA was loaded onto a tobramycin affinity column with 1 mL of buffer. The tobramycin affinity column was prepared as previously reported (*7*). The unbound RNA was eluted in the first three column volumes, whereas RNA bound specifically to the column was eluted with 10 mM tobramycin. The eluted RNAs were precipitated with ethanol, cleaved at the modified positions by aniline, and analyzed on 15% polyacrylamide/8 M urea gel. Alkaline hydrolysis ladders and RNase T1 sequencing ladders were included on the gels to permit identification of individual bands.

Ethylation Modification Interference Assays. 5′-^{32}P-labeled J6f1 RNA (2×10^6 cpm) was modified with ethylnitrosourea (ENU) under denaturing condition as described (*14*). After modification, the RNA was precipitated with ethanol and lyophilized. Two pools of RNA, tobramycin-bound and unbound RNAs, were separated in the same way as described before. To cleave RNAs at the modified phosphate, RNAs were resuspended in 20 μL of 100 mM triethylammonium bicarbonate, pH 9.0, and heated at 50 °C for 5 min. RNAs were then lyophilized and analyzed on 15% polyacrylamide/8 M urea gels.

Ce(III) ion Mediated Footprinting Assay. 5′-^{32}P-labeled J6f1 RNA (1×10^6 cpm) was incubated with 1 mM cerium(III) nitrate hexahydrate in the presence or absence of 1 μM tobramycin for 8 h at 25 °C. The RNA was precipitated with ethanol and analyzed on 15% polyacrylamide/8 M urea gel.

DEPC Probing of Mutant J6f1 RNAs. 5′-^{32}P-labeled RNA (1×10^5 cpm) in 100 μL of buffer solution containing 140 mM NaCl, 5 mM KCl, 1 mM $MgCl_2$, 1 mM $CaCl_2$, and 20 mM HEPES (pH 7.4) was treated with 10 μL of DEPC at 25 °C for 1 h. The RNA was precipitated with ethanol, cleaved at the modified positions by aniline, and analyzed on 15% polyacrylamide/8 M urea gel.

Fluorescence Measurements. Tetramethylrhodamine labeled tobramycin (CRT), concentrations were determined spectroscopically at 550 nm using a molar extinction coefficient of 6.00×10^4 M^{-1} cm^{-1}. Fluorescence anisotropy measurements were performed on a Perkin-Elmer LS-50B luminescence spectrometer equipped with a thermostat accurate to ±0.1 °C. The tracer solution was excited at 550 nm and monitored at 580 nm. The integration time was 10 s. For every single point, 6 measurements were made, and their average values were used for calculation. Measurements were performed in buffer solution containing 140 mM NaCl, 5 mM KCl, 1 mM $MgCl_2$, 1 mM $CaCl_2$, and 20 mM HEPES (pH 7.4).

Determination of Dissociation Constants. The following eq 1 was used for the determination of the dissociation constant for the interactions between RNA and CRT (K_d):

$$A = A_0 + \Delta A\,[([\mathrm{RNA}]_0 + [\mathrm{CRT}]_0 + K_d) - (([\mathrm{RNA}]_0 + [\mathrm{CRT}]_0 + K_d)^2 - 4[\mathrm{RNA}]_0[\mathrm{CRT}]_0)^{1/2}]/2 \quad (1)$$

where A and A_0 are the fluorescence anisotropy of CRT in the presence and in the absence of RNA, respectively. ΔA is the difference between the fluorescence anisotropy of 1 nM of CRT in the presence of an infinite concentration of RNA and the fluorescence anisotropy in the absence of RNA. $[\mathrm{RNA}]_0$ and $[\mathrm{CRT}]_0$ are the initial concentrations of RNA and CRT, respectively.

In the competitive binding assay, eq 2 is used for the calculation of the K_D values:

$$[\text{aminoglycoside}]_0 = [K_D\,(A_8 - A)/K_d\,(A - A_o) + 1] \times ([\mathrm{RNA}]_0 - K_d(A - A_o)/(A_8 - A) - [\mathrm{CRT}]_0(A - A_o)/(A_8 - A_o)) \quad (2)$$

where K_D is the dissociation constant between the RNA and the aminoglycosides. $[\text{aminoglycoside}]_0$ is the initial concentration of the aminoglycosides. Both K_d and K_D were determined by nonlinear curve fitting using the equations described above (*2*).

RESULTS

Chemical Modification Interference Using DEPC and Hydrazine. Chemical modification interference assays (*15*) were used to investigate which nucleotides are important for

[1] Abbreviations: DEPC, diethyl pyrophosphate; ENU, ethylnitrosourea; CRT, tetramethylrhodamine labeled tobramycin; nt, nucleotide.

tobramycin binding to J6f1 RNA. The 5′-end labeled J6f1 RNA was modified under denaturing conditions using diethyl pyrocarbonate (DEPC) and hydrazine. We chose DEPC and hydrazine for the chemical modification because these reagents modify the base moieties and may interfere with base-specific recognition by tobramycin. DEPC is a reagent designed to carboxyethylate the N-7 position of adenosine and, to a lesser extent, guanosine residues (*13*). This modification results in the opening of the purine imidazole ring and, therefore, should interfere with tobramycin-RNA interaction. Hydrazine modifies the pyrimidine bases (U and C) by nucleophilic attack at the pyrimidine 5,6 double bond (*13*). Modification by hydrazine can abolish potential Watson−Crick base pairing, whereas DEPC modification does not interfere with base pairing. Modification interference using these reagents can identify bases that are specifically involved in the tobramycin interaction.

Modified RNAs were loaded onto a tobramycin affinity column and were eluted with the tobramycin binding buffer. The unbound RNA was eluted in the first three column volumes, whereas RNA bound specifically to the column eluted with 10 mM tobramycin. Tobramycin-bound and unbound RNAs were cleaved with aniline and run on gels. Comparison of band intensities between bound and unbound RNAs identifies sites of modifications that interfere with tobramycin binding.

As shown in Figures 1 and 2, modification of five consecutive bases, G14−U18, by DEPC and modification of U18, U19, and U20 by hydrazine abolished tobramycin binding. By contrast, modification of the three nucleotide bulge did not interfere with tobramycin binding. Unfortunately, it has not been possible to determine whether the single base bulge (A27) is directly involved in tobramycin binding because this base was not modified with DEPC, even under denaturing conditions. In addition, although DEPC is known to react specifically with purine bases (*13*), several pyrimidines are modified (Figure 1). Reactions of DEPC with pyrimidine residues are poorly understood, but not unknown (*16*−*18*). On the basis of these results, it appears most likely that tobramycin binds to the stem-loop region, centered at the single base bulge of J6f1 RNA.

Probing the Structure of Mutant J6f1 RNAs with DEPC. Previous studies have shown that deletion of either a three nucleotide bulge (A9 U10 A11) or an one nucleotide bulge (A23) from J6f1 RNA abolished high-affinity and stoichiometric tobramycin binding (*10*). To test whether the removal of these bulges result in a structural change in the duplex region of J6f1 RNA, mutant RNA structures were probed using the DEPC accessibility assay. Neither J6f2 nor J6f3 specifically bind tobramycin (*10*).

Diethyl pyrocarbonate (DEPC) is a small chemical probe with a ∼3.5 Å diameter, which is comparable to the width of the major groove in an A-form RNA helix (*19*). Purine bases in canonical Watson−Crick base pairing are generally unreactive toward DEPC because N-7 positions are buried deep in the narrow major groove of the RNA helix (*17*, *20*). Therefore, the DEPC reactivity rates reflect the steric accessibility of purine bases in the major groove (*18*, *19*).

As shown in Figure 3, U20−G22 bases in the loop sequence were comparably modified with DEPC in each RNA. This is a useful control to ensure that each RNA experienced similar carboxyethylation conditions. As expected, purine bases in the loop regions of each RNA are highly accessible to DEPC. By contrast, modifications in the other regions show different patterns for each RNA. In J6f1, only the weak modification is observed at G17 in the duplex region. J6f2 shows DEPC reactivity at G10 in the three nucleotide bulge, whereas enhanced reactivity is observed at four bases flanking a single base bulge in J6f3. These results suggest that two bulges have significant effects on the specific conformation of duplex regions of J6f1.

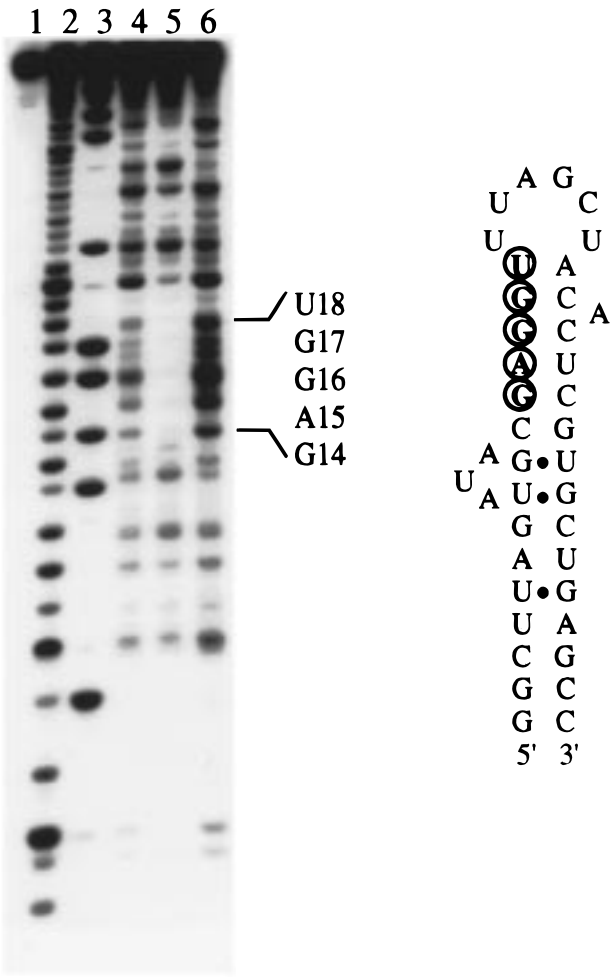

FIGURE 1: Diethyl pyrocarbonate (DEPC) modification interference of tobramycin binding to J6f1 RNA. Autoradiogram of a 15% denaturing polyacrylamide gel showing DEPC modification of 5′-^{32}P-labeled J6f1 RNA. (Lane 1) Intact J6f1 RNA; (lane 2) alkaline hydrolysis; (lane 3) G-specific RNase T1 sequencing reaction; (lane 4) DEPC control reaction; (lane 5) bound RNA; (lane 6) unbound RNA. Modified sites which interfered with the binding of tobramycin are shown in open circles on the secondary structure of J6f1 RNA.

Lack of Interaction of the Phosphate Backbone of J6f1 with Tobramycin. To identify possible phosphate contacts with tobramycin, we performed an ethylation interference experiment with tobramycin. Ethyl nitrosourea (ENU) is known to react with phosphate residues of nucleic acids (*14*). Surprisingly, strong interference by ethyl nitrosourea was not observed with the phosphate backbone of J6f1 RNA as shown in Figure 4A. To confirm this result, a Ce(III) ion-mediated footprinting experiment was performed. Ce(III) ion is known to bind to the phosphate groups of RNA, and cleave the RNA backbone at neutral pH (*21*). As shown in Figure 4B, the cleavage patterns of phosphate backbone by

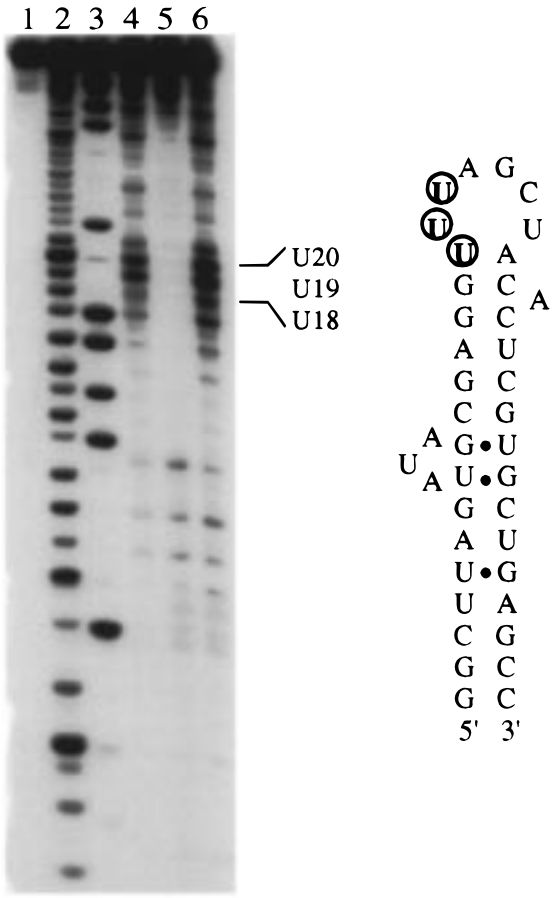

FIGURE 2: Hydrazine modification interference of tobramycin binding to J6f1 RNA. Autoradiogram of a 15% denaturing polyacrylamide gel showing hydrazine modification of 5′-^{32}P-labeled J6f1 RNA. (Lane 1) Intact J6f1 RNA; (lane 2) alkaline hydrolysis; (lane 3) G-specific RNase T1 sequencing reaction; (lane 4) hydrazine control reaction; (lane 5) bound RNA; (lane 6) unbound RNA. Modified sites which interfered with the binding of tobramycin are shown in open circles on the secondary structure of J6f1 RNA.

Ce(III) ion was not altered by the presence of 1 μM tobramycin. These results suggest that there might not be specific interactions between tobramycin and the phosphate groups of J6f1.

Mutational Studies on J6f1 RNA. To further investigate the importance of specific bases, a series of mutations, shown in Scheme 2, were introduced into J6f1 RNA. Three different sets of mutations were studied. Mutations in the duplex regions are identified in the J6fd series. Mutations in the loop region are identified in the J6fl series, and finally, mutations in the bulge regions are identified in the J6fb series. The mutational series is illustrated in Scheme 2. A summary of binding of CRT and tobramycin to these RNAs is shown in Table 1. Representative binding isotherms for each series are shown in Figure 5: J6fd6 (saturable and stoichiometric binding), J6fl1 (no specific binding), and J6fb1 (no specific binding).

Mutations of Watson−Crick base pairs in the stem region (J6fd series) were done by reversing each base pair or changing one base from each base pair to maintain the nucleotide composition and base-pairing stability of the stem region. All the mutations of the base pairs, except for substitution of G14·C30 with a G·U pair, had significant effects on CRT binding (Table 1). Most mutations abolished specific CRT binding altogether, whereas mutations of the A15·U29, G17·C26, and U18·A25 base pairs (to U·A/A·C, G·U, and U·G pairs) showed nonstoichiometric binding with CRT.

A series of mutations in the loop region (J6fl series) were also tested to examine the local sequence requirement for binding. U19, U20, and U24 bases are critical for the CRT binding (Table 1). By contrast, A21, G22, and C23 could be mutated to other bases with little effect on binding. This is the expected result given the chemical interference data.

Mutations of the single base bulge A27 to G or U (J6fb series) also abolished specific CRT binding. It appears that identity of the single base bulge A27 may be critical for tobramycin binding. These results are consistent with the chemical interference data. Thus, the single base bulge and stem regions appear to be critical for the tobramycin binding. We previously reported that elimination of the three nucleotide bulge (A9 U10 A11) eliminated specific CRT binding (*10*). However, chemical interference data shown in Figures 1 and 2 suggest that tobramycin may not directly contact the three nucleotide bulge. To confirm the role of this bulge in tobramycin binding, the sequence A9 U10 A11 was replaced by a UUU sequence (J6b3, Table 1). This mutant sequence showed weak, nonstoichiometric binding with CRT (Figure 6). In addition, mutation of two wobble base pairs (G12·U32 and U8·G33) to canonical Watson−Crick base pairs (G·C and C·G) showed similar nonstoichiometric binding with CRT (Table 1). This result is consistent with the idea that the three nucleotide bulge sequence and the adjacent wobble base pairs are important structurally for specific interactions with tobramycin**.**

DISCUSSION

Previous studies from this laboratory have shown that high-affinity and specific RNA aptamers can be selected against the aminoglycoside tobramycin (*7*). The binding affinities of these aptamers for aminoglycosides can be accurately determined by fluorescence measurements (*7, 11*). In the current studies, fluorescence anisotropy was used to monitor the interactions of CRT with the RNA constructs (*10*). Direct competition experiments between CRT and various aminoglycosides are used to determine dissociation constants between the aminoglycosides and the RNA constructs (*7, 10, 11*). J6 is one of the high affinity RNA aptamers that has been generated by selection (*7*). The full J6 structure could be reduced in size to generate J6f1 (Scheme 1), which still binds tobramycin specifically and with high affinity (*10*). As expected, this doubly bulged stem-loop structure contains the consensus sequence of the selected aptamers which bind to tobramycin (*10*). The object of the studies reported here is to determine where the tobramycin binding site resides in J6f1. This kind of study is particularly useful for informing anticipated structural studies on the nature of the aminoglycoside binding site in the aptamer.

Chemical interference studies were used to investigate which nucleotides are important for tobramycin binding. In this approach, the denatured RNA molecule is first modified with a reagent under conditions where, on average, there is less than one modification per RNA molecule (*15*). Renaturation of the RNA molecules, followed by affinity chromatography, separates tobramycin binding and nonbinding

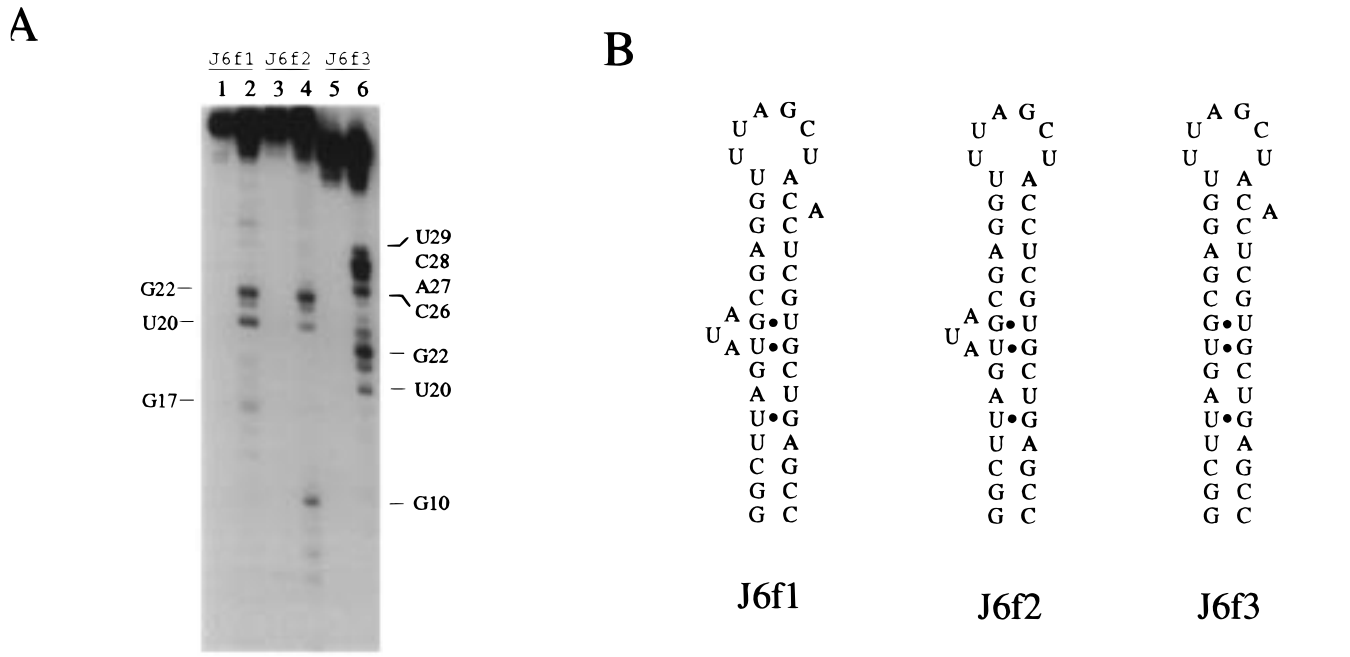

FIGURE 3: DEPC accessibility experiments. (A) Autoradiogram of an 15% denaturing polyacrylamide gel showing DEPC modification of 5′-^{32}P-labeled J6f1 RNA. (Lane 1) Intact J6f1 RNA; (lane 2) DEPC-treated J6f1 RNA; (lane 3) intact J6f2 RNA; (lane 4) DEPC-treated J6f2 RNA; (lane 5) intact J6f3 RNA; (lane 6) DEPC-treated J6f3 RNA. (B) Predicted secondary structures of RNAs used in this experiment.

RNA molecules. Determination of which nucleotides are modified allows one to access the roles of these nucleotides in antibiotic binding. While it is generally assumed that this technique probes direct interactions between a particular probe and RNA, it is also possible that chemical modification may change the tertiary structure of RNA and thereby indirectly interfere with ligand binding. However, this methodology is far more informative than direct chemical protection experiments using binding ligands and modifying agents simply because the modifying agents are generally incapable of reacting with nucleotides that are base paired.

When the chemical interference methodology was applied to J6f1 with DEPC or hydrazine, internally consistent and clear results were obtained. DEPC modification of five consecutive bases (G14−U18) interfered with tobramycin binding. Moreover, modification of three consecutive uridines (U18−U20) by hydrazine also led to abolition of tobramycin binding. Modification of the three nucleotide bulge did not result in interference with tobramycin binding. On the basis of these results, it would appear that tobramycin binds to the stem-loop region centered at the single base bulge of J6f1. The proposed binding site for J6f1 is shown in Figure 7.

It is interesting to compare the DEPC modification patterns of J5f1 to J6f2 and J6f3. These latter RNA molecules do not show high-affinity, saturable binding to tobramycin (*10*), meaning that the structure of the tobramycin binding sites differs from that found in J6f1. The purine bases in the loop regions of each RNA are highly accessible to DEPC, while modifications in the other regions show different patterns for each RNA. These results are in accord with the idea that the two bulges have significant effects on the specific conformation of duplex regions of RNA in the J6f series.

One plausible mode of aminoglycoside-RNA recognition is through electrostatic interactions between the positively charged amino groups of the aminoglycoside and the phosphate backbone of the RNA. To probe this possibility,

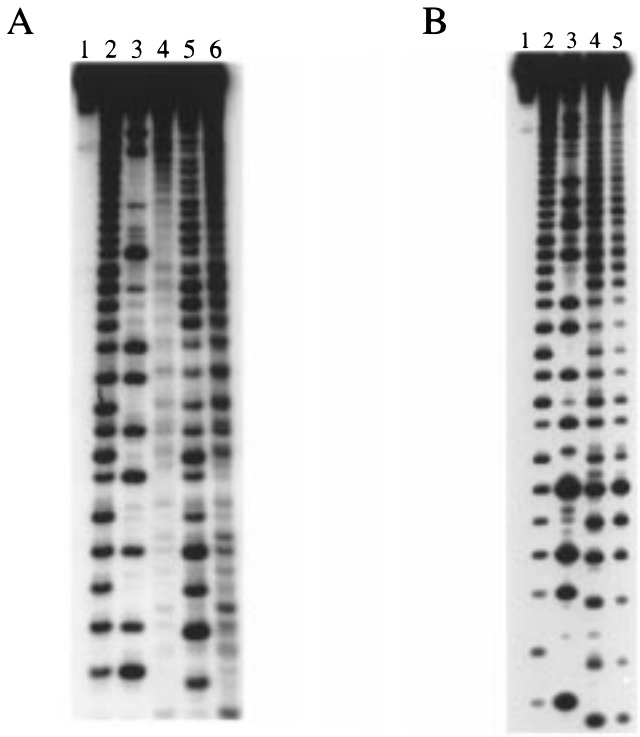

FIGURE 4: Probing the specific interaction between tobramycin and phosphate backbone of J6f1 RNA. (A) Autoradiogram of a 15% denaturing polyacrylamide gel showing ethyl nitrosourea (ENU) modification interference of 5′-^{32}P-labeled J6f1 RNA. (Lane 1) Intact J6f1 RNA; (lane 2) alkaline hydrolysis; (lane 3) G-specific RNase T1 sequencing reaction; (lane 4) ENU control reaction; (lane 5) bound RNA; (lane 6) unbound RNA. (B) Autoradiogram of an 15% denaturing polyacrylamide gel showing Ce(III) ion-mediated footprinting of 5′-^{32}P-labeled J6f1 RNA. (Lane 1) Intact J6f1 RNA; (lane 2) alkaline hydrolysis; (lane 3) G-specific RNase T1 sequencing reaction; (lane 4) Ce(III) ion-mediated cleavage control reaction; (lane 5) Ce(III) ion-mediated cleavage reaction in the presence of 1 μM tobramycin.

Scheme 2: A Series of Mutations in J6F1 RNA; (A) Mutations in the Duplex Region J6F1 (J6fd1-J6fd10), (B) Mutations in the Loop Region of J6F1 (J6fl1-J6fl8), and (C) Mutations in the Bulge Region of J6F1 (J6fb1-J6fb4)

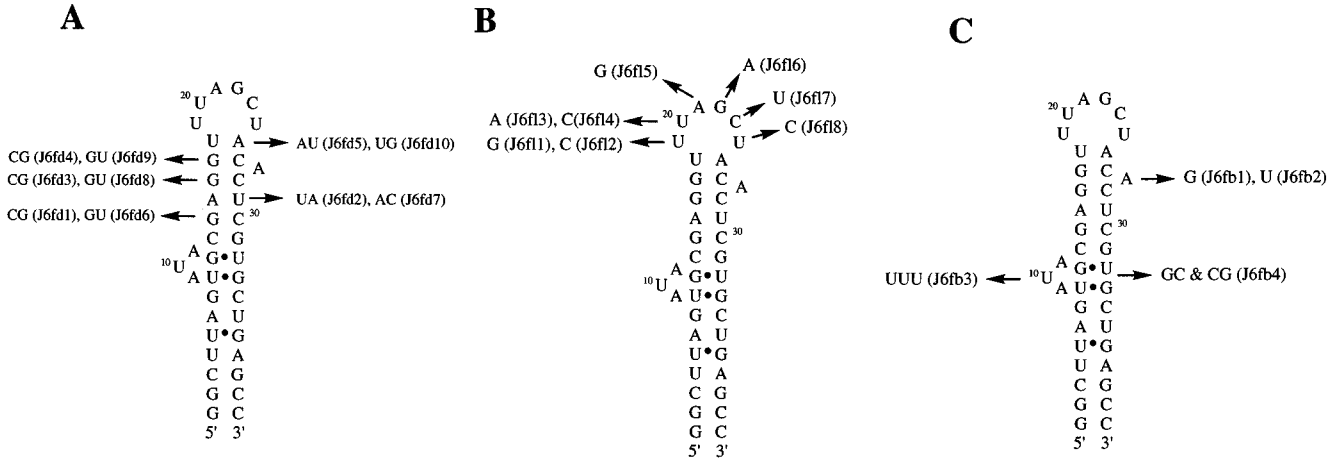

Table 1: CRT- and Tobramycin-Binding Studies of J6f1 Mutant RNAs

mutant	original	mutation	CRT K_d (nM)	tobramycin K_D (nM)
J6f1			192.6 ± 11.1	5.15 ± 1.52
J6fd1	G14·C30	C14·G30	nb[a]	
J6fd2	A15·U29	U15·A29	ns[b]	
J6fd3	G16·C28	C16·G28	nb	
J6fd4	G17·C26	C17·G26	nb	
J6fd5	U18·A25	A18·U25	nb	
J6fd6	G14·C30	G14·U30	148 ± 80	34.0 ± 0.9
J6fd7	A15·U29	A15·C29	ns	
J6fd8	G16·C28	G16·U28	nb	
J6fd9	G17·C26	G17·U26	ns	
J6fd10	U18·A25	U18·G25	ns	
J6f11	U19	G19	nb	
J6f12	U19	C19	nb	
J6f13	U20	A20	nb	
J6f14	U20	C20	nb	
J6f15	A21	G21	425.8 ± 40.9	18.99 ± 1.99
J6f16	G22	A22	60.5 ± 2.3	2.55 ± 0.25
J6f17	C23	U23	420.4 ± 65.4	18.81 ± 0.59
J6f18	U24	C24	nb	
J6fb1	A27	G27	nb	
J6fb2	A27	U27	nb	
J6fb3	A9 U10 A11	U9 U10 U11	ns	
J6fb4	U8·G33	C8·G33	ns	
	G12·U32	G12·C32		

[a] nb, nonspecific binding. [b] ns, nonstoichiometric binding.

ethylation interference experiments were performed with ENU. No strong interference patterns were observed, suggesting that the phosphate backbone is not involved in recognition. Ce(III)-ion-mediated footprinting experiments are also consistent with this idea. The Ce(III)-mediated cleavage pattern was not perturbed by tobramycin, suggesting that phosphate moieties are not part of the aminoglycoside binding domain. This is in contrast to other studies showing that the neomycin inhibition of a hammer-head ribozyme is strongly dependent on ionic interaction between the aminoglycoside and the RNA phosphate moieties (*22*). However, the binding of neomycin to the hammerhead occurs in the micromolar range (*22*). We suspect that weak aminoglycoside binding of this type will often involve electrostatic interactions mediated through phosphate groups. It appears that the structural basis of tobramycin-J6f1 recognition, which involves high-affinity interactions, is distinct from weak aminoglycoside−RNA interactions generally described.

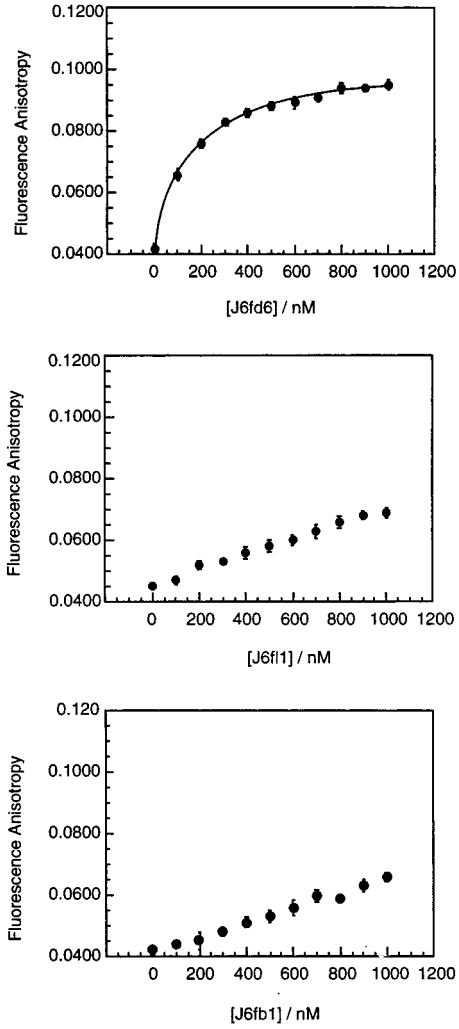

FIGURE 5: Representative binding isotherms for J6f1 mutants.

In aggregate, then, the experiments described here are consistent with the proposal that the stem-loop region of J6f1 is an important part of the tobramycin binding site. Mutational studies also support this hypothesis.

Since the chemical interference studies identified a portion of the Watson−Crick base paired stem as part of the aminoglycoside binding-site, it was of interest to probe this region by mutational analysis. Initial mutational studies were

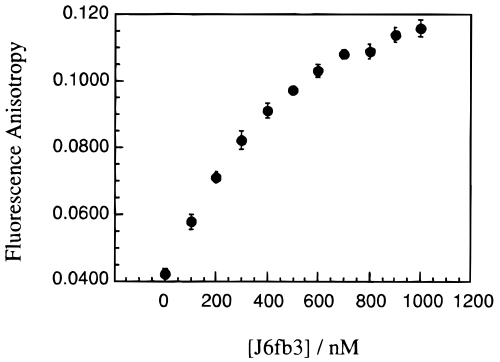

FIGURE 6: Fluorescence anisotropy of CRT (10 nM) solution as a function of J6fb3 RNA concentration.

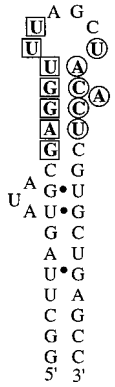

FIGURE 7: Proposed binding sites for tobramycin. Tobramycin-binding bases which are identified by chemical interference experiments are indicated in open box. Tobramycin-binding bases which are identified by mutation studies are indicated by open circles.

performed by reversing the bases in the critical part of the stem-loop, maintaining Watson−Crick base pairing. As expected from the chemical interference assays, none of these mutants specifically bound tobramycin. These results strongly imply that tobramycin is recognizing the nucleotide bases themselves.

Single base substitution studies were also performed. With the notable exception of the substitution of G14•C30 with a G•U base pair, all other single base substitutions led either to no aminoglycoside binding or to nonstoichiometric binding. Further interesting mutations are found in the bulge regions. Previous studies showed that the bulge regions are essential for high-affinity, specific binding of aminoglycosides (*10*). Here, it is shown that mutations of the single base bulge A27 to G or U abolishes aminoglycoside binding. This result is, of course, consistent with previous studies (*10*) and the chemical interference data described here and demonstrates the importance of the single base bulge for tobramycin binding. The three nucleotide bulge is also of substantial interest because elimination of this bulge eliminates aminoglycoside binding (*10*). Moreover, as shown here, replacement of the AUA sequence by UUU leads to a construct unable to specifically bind aminoglycosides. However, chemical interference data suggest that tobramycin does not directly interact with the nucleotides in this bulge. This could argue that this bulge is structurally important for aminoglycoside binding, without actually being part of the binding site. One possibility is that the bulge forces open the narrow A-form helical groove of the RNA allowing access to the aminoglycoside.

A final series of mutational studies probed the roles of the loop nucleotides in tobramycin binding, While U19, U20, and U24 are critical for binding, A21, G22, and C23 could be mutated to produce constructs which were still capable of specifically binding tobramycin.

On the basis of our results, tobramycin−J6f1 RNA interactions may be different from other aminoglycoside−RNA interactions. While most of the aminoglycoside-binding RNA molecules described so far appear bind aminoglycosides in the micromolar range, J6f1 RNA binds tobramycin in the nanomolar range. Aminoglycosides are polycationic at neutral pH, and therefore, ionic interactions between the positively charged amino groups of aminoglycosides and negatively charged phosphate groups of RNA can be important for aminoglycoside binding (*22*, *23*). However, these kinds of electrostatic interactions may not result in binding of the high-affinity (nM) type.

In summary, the experiments reported here reveal those parts of the stem-loop domain of J6f1 which make up the tobramycin binding site. Specific interactions of the aminoglycoside with the phosphate backbone of the RNA are apparently not important for binding. It appears that specific interactions do occur between tobramycin and certain nucleotides in the stem-loop region. The trinucleotide bulge appears to be essential for maintaining the correct overall structure of the tobramycin binding site, without actually being part of the binding site.

REFERENCES

1. Chambers, H. F., and Sande, M. A. (1996) *Goodman & Gilman's The Pharmacological Basis of Therapeutics*, p 1103, McGraw-Hill Companies, New York.
2. Noller, H. F. (1991) *Annu. Rev. Biochem. 60*, 191−227.
3. De Stasio, E. A., and Dahlberg, A. E. (1990) *J. Mol. Biol. 212*, 127−133.
4. von Ahsen, U., Davis, J., and Schroeder, R., (1991) *Nature 353*, 368−370.
5. Stage, T. K., Hertel, K. J., and Uhlenbeck, O. C. (1995) *RNA* 1, 95−101.
6. Zapp, M. L., Stern, S., and Green, M. R. (1993) *Cell 74*, 969−978.
7. Wang, Y., and Rando, R. R. (1995) *Chem. Biol. 2*, 281−290.
8. Lato, S. M., Boles, A. R., and Ellington, A. D. (1995) *Chem. Biol. 2*, 219−303.
9. Wallis, M. G., von Asen, U., Schroeder, R., and Famulok, M. (1995) *Chem. Biol. 2*, 543−552.
10. Hamasaki, K., Killian, J., Cho, J., and Rando, R. R. (1997) *Biochemistry 36*, 1367−1371.
11. Wang Y., Killian, J., Hamasaki, K., and Rando, R. R. (1996) *Biochemistry 35*, 12338−12346.
12. Milligan, J. F., and Uhlenbeck, O. C. (1989) *Methods Enzymol. 180*, 51−62.
13. Peattie, D. A. (1979) *Proc. Natl. Acad. Sci. U.S.A. 76*, 1760−1764.
14. Calnan, B. J., Tidor, B., Biancalana, S., Hudson, D., and Frankel, A. D. (1991) *Science 252*, 1167−1171.
15. Conway, L., and Wickens, M. (1989) *Methods Enzymol. 180*, 369−379.
16. Van Stolk, B. J., and Noller, H. F. (1984) *J. Mol. Biol. 180*, 151−177.
17. Mougel (1987) *Science 261*, 1574−1577.
18. Weeks, K. M., and Crothers, D. M. (1991) *Cell 66*, 577−588.
19. Weeks, K. M., and Crothers, D. M. (1993) *Science 261*, 1574−1577.
20. Peattie, D. A., and Gilbert, W. (1980) *Proc. Natl. Acad. Sci. U.S.A. 77*, 4679−4682.

21. Baumann, E., Trapman, H., and Fischler, F. (1954) *Biochem. Z. 328*, 89−96.
22. Clouet-d′Orval, B., Stage, T. K., and Uhlenbeck, O. C. (1995) *Biochemistry* 34, 11186−11190.
23. Fourmy, D., Recht, M. I., Blanchard, S. C., and Puglisi, J. D. (1996) *Science 274*, 1367−1371.

BI972757H